Investigations on structural, optical and electrical properties of V_2O_5 nanoparticles

Khushal Sagapariya, K. N. Rathod, Keval Gadani, Hetal Boricha, V. G. Shrimali, Bhargav Rajyaguru, Amiras Donga, A. D. Joshi, D. D. Pandya, N. A. Shah, and P. S. Solanki

Citation: AIP Conference Proceedings **1837**, 030006 (2017); doi: 10.1063/1.4982084
View online: http://dx.doi.org/10.1063/1.4982084
View Table of Contents: http://aip.scitation.org/toc/apc/1837/1
Published by the American Institute of Physics

Investigations on Structural, Optical and Electrical Properties of V_2O_5 Nanoparticles

Khushal Sagapariya[1], K.N. Rathod[1], Keval Gadani[1], Hetal Boricha[1], V.G. Shrimali[1,2], Bhargav Rajyaguru[1], Amiras Donga[1], A.D. Joshi[3], D.D. Pandya[4], N.A. Shah[1], P.S. Solanki[1,a)]

[1]*Department of Physics, Saurashtra University, Rajkot – 360 005, India*
[2]*Government Polytechnic, Gujarat Technological University, Rajkot – 360 003, India*
[3]*Department of Nanoscience and Advanced Materials, Saurashtra University, Rajkot – 360 005, India*
[4]*Human Resource & Development Centre, Saurashtra University, Rajkot – 360 005, India*

[a)]E–mail: piyush.physics@gmail.com

Abstract. In present communication, structural, optical and electrical properties of nanostructured vanadium pentoxide (V_2O_5) have been investigated. UV–Visible spectroscopy measurements were carried out in order to investigate the optical properties of as grown V_2O_5 samples. UV–Visible absorption spectrum shows a shifting in absorption peak towards lower wavelength from pure to different concentrated as grown samples. Value of optical band–gap (E_g), estimated from optical measurements, increases from 2.89 to 3.38eV with increase in concentration. Nanostructured V_2O_5 samples were synthesized using cost effective sol–gel method and final product was sintered at different temperatures. X–ray diffraction (XRD) measurement was performed to investigate the structural phases present which revealing the single phasic nature with orthorhombic structure. Crystallite size (CS), calculated using Scherer's formula, is found to be ~ 38.13 for 500°C sintered sample which increases to ~ 51.31nm for higher temperature sintered sample. Improved CS leads to the decrease in crystal boundary density in the sample sintered at higher temperature. Electrical properties of nanostructured V_2O_5 were studied by carrying out dielectric and A.C. conductivity measurements. Dielectric and A.C. conductivity have been understood on the basis of CS, crystal boundaries and interaction between the mobile ions and lattice in the nanoparticles.

INTRODUCTION

Vanadium pentoxide (V_2O_5) is very interesting since it is a fine catalyst and can be utilized in many potential applications. It is n–type semiconducting material with a wide band–gap (E_g) of ~ 2.2–2.3eV [1,2] and has interesting electrochemical performances [3,4]. Due to its multivalence nature, layered structure, wide optical band–gap, good chemical and thermal stability and excellent thermoelectric properties, nowadays, V_2O_5 becomes a promising material for applications in microelectronics, optoelectronic devices, solar cell, electrochromic devices, electronic switches, optical switches, etc [5–9].

Dielectric and A.C. conductivity properties of V_2O_5 based composites were studied over a broad range of frequency and temperature by Kattimani et al [10]. Effect of vanadium pentoxide (V_2O_5) on the electrical, dielectric and optical properties of polyvinyl alcohol (PVA) / V_2O_5 nanocomposites was investigated by Nabil Shash [11]. Shash has found that the dielectric and electrical properties of the nanocomposite films get improved through the addition of V_2O_5 [11]. Conductivity of molten V_2O_5 was investigated by Allersma [12] on the basis of dissociation of V_2O_5 with variation in partial pressure. Correlated electrons are responsible for the extreme sensitivity of materials for small change in external stimuli such as pressure, temperature or doping [13]. Doping is one of the effective approaches for altering, controlling and tailoring the structural, optical and electrical properties of every semiconducting oxide. Different ions like W, Mo, Nb, F, Cr, Al and S have been examined for this purpose [14–18]. In a similar way, one can design various materials at nanoscale by employing different synthesis parameters such as sintering temperature, molarity concentration, pH, sintering time, sintering environment, etc.

In this communication, we report the study on optical studies for V_2O_5 material, by employing UV–Visible spectroscopy measurements on different concentrated V_2O_5 samples. Analysis of optical spectra was accomplished by solvent effects and electronic transitions. Also, the effect of sintering temperature on the

Functional Oxides and Nanomaterials
AIP Conf. Proc. 1837, 030006-1–030006-4; doi: 10.1063/1.4982084
Published by AIP Publishing. 978-0-7354-1507-2/$30.00

structural phase formation, dielectric constant and A.C. conductivity of V_2O_5 nanoparticles was studied on the basis of CS, boundary effect and possible interaction between the mobile ions and the lattice.

EXPERIMENTAL DETAILS

V_2O_5 nanostructures were synthesized using convectional sol–gel technique, in which ammonium vanadate (NH_4VO_3) precursor was dissolved in diluted ethanol (CH_3CH_2OH). In order to obtain homogeneous mixture, solution was stirred with continuous heat at 60°C. Optical properties of these as grown V_2O_5 samples were studied by carrying out UV–Visible spectroscopy using UV–Vis spectrometer (SPECORD 200 PLUS Anaytic Jena). UV-Visible measurements were performed in liquid phase. Double distilled water was used in which V_2O_5 is slightly soluble and then sonicator was used to get highly dispersed solution and finally used for UV-Visible measurements. As highly dispersed solution was used for UV-Visible measurements, it is possible to obtain transmission spectra. Then, solution was properly heated at higher temperatures, resulting in a fine powder. The powder was then crushed for 3h followed by calcination at 200°C for 2h. Sintering process was finally employed at 500 and 650°C temperatures for 2h under air environment. Structural phase was investigated using XRD measurements at room temperature by Philips diffractometer (PW 3040/60, X'pert Pro) using Cu Kα radiation. Electrical measurements, dielectric and A.C. conductivity, were carried out at room temperature using Agilent E4980A Precision LCR meter in the frequency range of 20Hz to 2MHz.

RESULTS AND DISCUSSIONS

Fig.1(a) shows XRD patterns of sol–gel grown vanadium pentoxide (V_2O_5) samples, sintered at 500 and 650°C temperatures. Fig.1(b) shows an enlarged view of most intense XRD peaks of the samples. Both the samples possess pure phase with orthorhombic unit cell structure without any detectable impurity within the range of 2θ as well as sintering temperature. Sample sintered at 650°C exhibits higher intensity of peaks as compared to the sample sintered at 500°C which implies better crystallinity of the sample sintered at higher temperature. Crystallite size (CS) of the samples was calculated using Scherer's formula and is found to be ~ 38.13 and 51.31nm for the samples sintered at 500 and 650°C, respectively. It is clear that CS increases with increase in sintering temperature mainly due to the agglomeration effect between the two or more smaller crystallites to form a larger one [19] and hence crystal boundary density gets suppressed in higher temperature sintered sample.

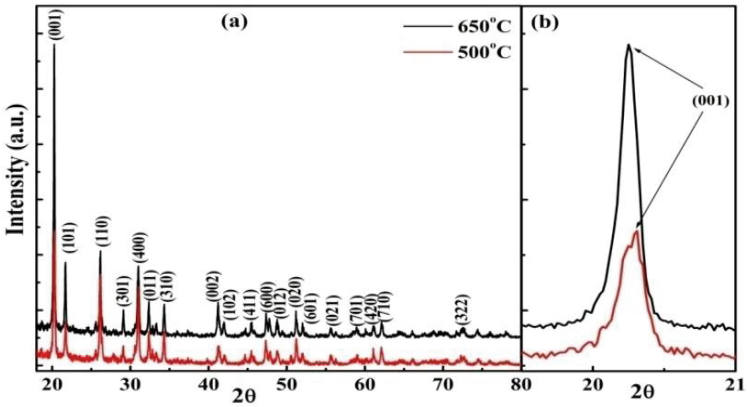

FIGURE 1. (a) XRD patterns of vanadium pentoxide (b) an enlarged view of most intense peaks of V_2O_5 sintered at different temperatures.

Fig.2(left) shows an absorption spectrum for the as grown V_2O_5 sample having different concentration. Pure sample (VO) exhibits absorption peak at ~ 0.346μm wavelength while other higher concentrate samples (VO1, VO2 and VO3) exhibit absorption peak at wavelength ~ 0.295μm. Shifting of absorption peak [Fig.2(left)] towards lower wavelength is due to the decrease in concentration of solvent and the blue shift may occur due to hydrogen bonding interaction [20] which gives rise to energy difference in different concentrated samples.

TABLE 1. Cut–off wavelength and band–gap variation for nanostructured V_2O_5.

Sample code	Cut–off wavelength λ_c (μm)	Band–gap (eV)
VO	0.4285	2.8993
VO1	0.3559	3.4907
VO2	0.3608	3.4433
VO3	0.3665	3.3898

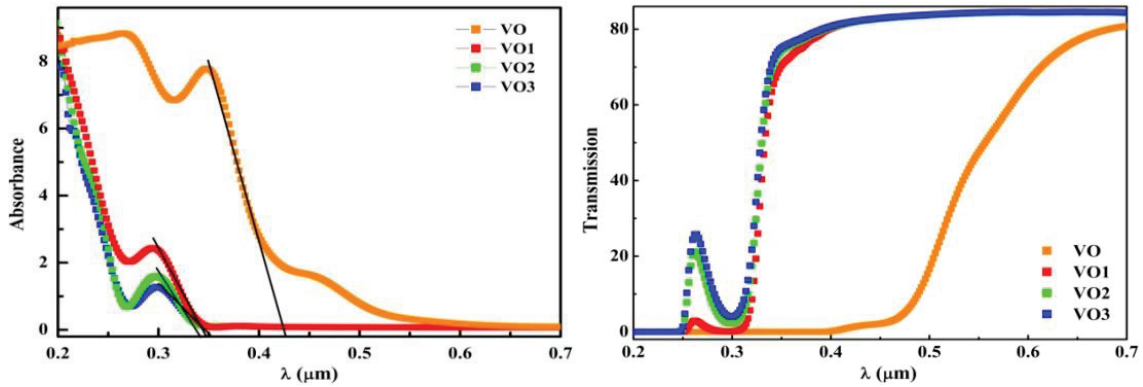

FIGURE 2. (left) Fits for cut–off wavelength and (right) Transmission spectrum for nanostructured V_2O_5.

No more vibrational energy levels are involved in all the samples, and hence, absorption peak does not show enough broadening. Intensity of the absorption peak varies from ~ 8 (for VO) to ~ 2 arbitrary units (for VO1, VO2 and VO3) because of the electronic transition exists since samples have reduction in their pH values from 8 to 4 for VO to VO3 samples, respectively.

Fig.2(left) shows the values of cut–off wavelengths for all the samples (indicated by the dark black straight–lines). Values of band–gap for all the different concentrated samples are shown in table 1 estimated using the equation: $E_g = hc / \lambda_c$, where E_g is the energy band–gap, h is the plank's constant = 6.626×10^{-34} J·sec, c is the light velocity = 3×10^{10} cm/sec and λ_c is the cut–off wavelength (in μm range). From the table 1, it is clear that energy band–gap decreases with increase in concentration of the samples which can be correlated with the decrease in cut–off wavelength. Refractive index is calculated using the two different equations: (i) $\eta = c/v$, where $c = 3 \times 10^{10}$ cm/sec and $v = 2.237 \times 10^{10}$ cm/sec and (ii) $\eta(\lambda) = 1.68606 + (51020.2 / \lambda^2)$ (Cauchy equation). Value of refractive index is found to be ~ 1.34 [from equation (i)], which is in agreement with the reported value by Tashtoush et al [21] and ~ 1.9 (from Cauchy equation).

Fig.2(right) shows UV–Visible transmission spectrum for all the as grown samples with different concentration in the solvent. Maximum transmittance ~ 84% in visible range can be observed for VO1, VO2, and VO3 samples while for VO, it is suppressed to ~ 80%. Transmittance peak observed well below 0.3μm for VO1, VO2, and VO3 samples is absent in VO indicating more absorbance in this sample.

Frequency dependent dielectric behavior for both the V_2O_5 nanostructured samples, sintered at two different temperatures, is shown in Fig.3(left). Inset of Fig.3(left) shows the variation in dielectric loss with frequency. Decrease in the value of dielectric constant with increasing frequency can be explained on the basis of reduced polarization and enhanced relaxation processes at higher frequency region. Electrical polarization in the dielectric materials is the sum of the contributions from dipolar, electronic, ionic and interfacial polarizations [22]. At low frequencies, all the polarizations respond easily to the time varying (A.C.) electric field while as the frequency of the electric field increases, different polarization contributions decreases, as a result, the net polarization of the material is suppressed which leads to the reduction in the value of dielectric constant [23].

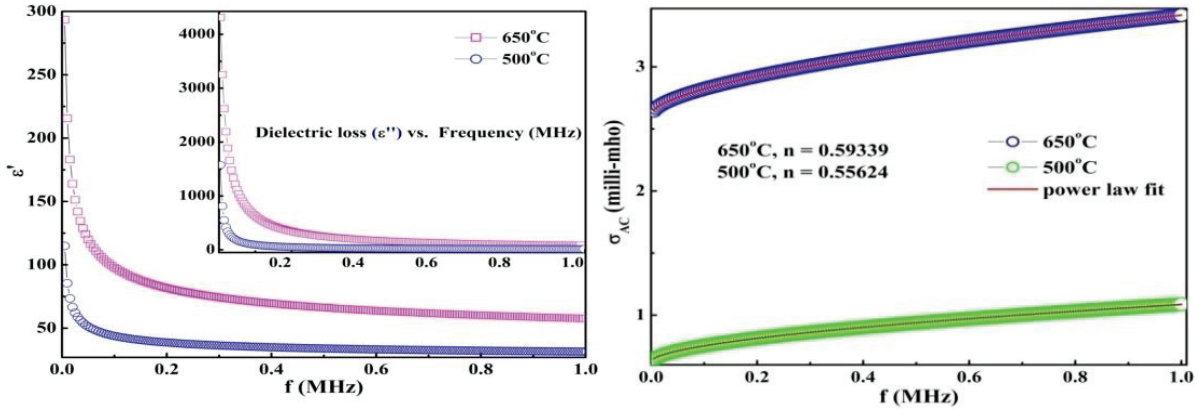

FIGURE 3. (left) Frequency dependent real dielectric constant and inset for imaginary dielectric constant and (right) frequency dependent A.C. conductivity with power law fits for nanostructured V_2O_5 sintered at different temperatures.

In similar way, dielectric loss is also found to decrease with increase in frequency, as shown in the inset of Fig.3(left). Large imaginary part of dielectric as compared to real one suggests that presently studied V_2O_5 nanoparticles possess effective loss nature may be due to disordered oxygen lattice. Increase in dielectric constant and electrical loss with increase in sintering temperature can be attributed to the enhanced CS and

reduced crystal boundary density which results in the interfacial electric / dipole polarization [22] and therefore dielectric constant gets enhanced in the sample sintered at higher temperature having larger CS and smaller boundary density.

Variation in A.C. conductivity with frequency for both the samples are shown in Fig.3(right). A.C. conductivity is found to increase with increase in frequency for both the samples as well as with sintering temperature. This may be due to the enhanced CS which leads to enlarged semiconducting cores and suppressed high resistive boundaries. For the case of present study, conductivity behavior obeys the universal power law [fits are shown in Fig.3(right)] [23]: $\sigma_{AC} = \sigma(0) + A\omega^n$, where $\sigma(0)$ is the D.C. conductivity, A is the temperature dependent coefficient, ω is the angular frequency of the applied A.C. field and n is the power law exponent. Power law exponent n signifies the interaction between the mobile ions and lattice in the samples. In present study, the values of power law exponent (n) are found to be ~ 0.55 and ~ 0.59 for V_2O_5 nanostructured samples sintered at 500 and 650°C, respectively. Value of power law exponent increases with increase in sintering temperature indicates an improved interaction between the mobile ions and lattice of the sample sintered at higher temperature.

CONCLUSIONS

In summary, UV–Visible spectroscopy shows a shifting in absorption spectrum for all the as grown samples (with different concentration in solvent) which has been understood in turns of the solvent effect and hydrogen bonding interaction. Change in the electronic transition brings out the alteration in absorption intensity of all the different concentrated samples. Band–gap energy and refractive index were estimated from the absorption spectrum. Structural studies using XRD measurement reveal the single phasic orthorhombic unit cell structure in both the samples grown by sol–gel technique and sintered at two different temperatures. Enhancement in dielectric constant with increase in sintering temperature has been understood in terms of CS, crystal boundary density and interfacial electric/dipole polarization. Increase in A.C. conductivity has been ascribed to the reduction in crystal boundary density in the sample sintered at higher temperature. Universal power law fits for conductivity data describe an interaction between the mobile ions and lattice of the samples which is stronger in the V_2O_5 nanoparticles synthesized at higher temperature.

REFERENCES

1. S.F. Cogan, N.M. Nguyen, S.J. Perrotti and R.D. Rauh, *J. Appl. Phys.* **66**, 1333 – 1337 (1989).
2. E.E. Chain, *Appl. Opt.* **30**, 2782 – 2787 (1991).
3. J.P. Pereira–Ramos, R. Messina and J. Perichon, *J. Appl. Electrochem.* **16**, 379 – 386 (1986).
4. H.K. Park, W.H. Smyrl and M.D. Ward, *J. Electrochem. Soc.* **142**, 1068 – 1073 (1995).
5. K.A. Cook–Chennault, N. Thambi and A.M. Sastry, *Smart Mater. Struct.* **17**, 043001: 1 – 33 (2008).
6. G.J. Fang, Z.L. Liu, Y.Q. Wang, H.H. Liu and K.L. Yao, *J. Phys. D: Appl. Phys.* **33**, 3018 – 3021(2000).
7. A.A. Akl, *J. Phys. Chem. Solids.* **71**, 223 – 229 (2010).
8. S.S. Kanu and R. Binions, *Proc. R. Soc.* **A 466**, 19 – 44 (2010).
9. F. Beteille and J. Livage, *J. Sol–Gel Sci. Technol.* **13**, 915 – 921 (1998).
10. J. Kattimani, T. Sankarappa, R. Ramanna and J. Ashwajeet, *Res. J. Chem. Sci.* **5**, 59 – 63 (2015).
11. N. Shash, *Ionics* **19**, 1825 – 1834 (2013).
12. T. Allersma, R. Hakim, T.N. Kennedy and J.D. Mackenzie, *J. Chem. Phys.* **46**, 154 – 160 (1967).
13. Kotliar G and Vollhardt D, *Phys. Today.* **57**, 53 – 60 (2004).
14. Z. Luo, Z. Wu, X. Xu, M. Du, T. Wang and Y. Jiang, *Mater. Sci. Eng. B.* **176**, 762 – 766 (2011).
15. M. Saeli, M.E. Warwick, C. Piccirllo and R. Binions, *Prop. Energy Consum. Model*. 117, 168 – 173 (2013).
16. B. Chen, D. Yang, P.A. Charpentier and M. Zeman, *Sol. Energy Mater. Sol. Cells.* **93**, 1550 – 1554 (2009).
17. P. Kiri, M.E. Warwick, I. Ridley and R. Binions, *Thin Solid Films.* **520**, 1363 – 1366 (2011).
18. M. Mousavi, A. Kompany, N. Shahtahmasebi and M. Bagheri–Mohagheghi, *Phys. Scr.* **88**, 65701: 1 – 5 (2013).
19. P.S. Solanki, R.R. Doshi, U.D. Khachar, M.V. Vagadia, A.B. Ravalia, D.G. Kuberkar and N.A. Shah, *J. Mater. Res.* **25**, 1799 – 1802 (2010).
20. M. Homocianu, A. Airinei and D. O. Dorohoi, *J. Adv. Res. Phys.* **2**, 011105: 1 – 9 (2011).
21. N. M. Tashtoush and O. Kasasbeh, *Jord. J. Phys.* **6**, 7 – 15 (2013).
22. N. A. Shah, *Appl. Nanosci* **4**, 889 – 895 (2014).
23. S. Sumi, P. Prabhakar Rao, M. Deepa and P. Koshy, *J. Appl. Phys.* **108**, 063718: 1 – 9 (2010).